DEVELOPMENT OF FLIGHT MECHANICAL MODELS AND CONTROL LAWS FOR THE AUTONOMOUS HELIPCOPTER SKELDAR

Per Weinerfelt, Ola Härkegård and Erik Backlund
Saab Aerosystems, Flight Physics
SE-58188 Linköping
Keywords: *Aerodynamics, Flight test, Optimization*

Abstract

The objective of this paper is to present simulation models and the design of control laws for the helicopter Skeldar V150. The simulation models include rotor dynamics, flight mechanics and the coupling between these equations and the rotor mechanism. The models, which are derived from fundamental physical laws, have been implemented in the symbolic mathematical software Maple which enables an efficient procedure for model analysis and simplifications of the governing equations together with automatic code generation.

A black box version of the dynamic equations, which were used both for the initial development of the control laws and for the validation of the models above, has been constructed using system identification. The black box models, which describe the roll, pitch and roll motions and the translation velocities, consist of simple linear systems having parameters which are identified from flight test data, mainly data from hovering conditions.

Comparisons between the nonlinear simulation model, a linearized version, the black box version and flight test data are presented in the results section in this paper.

1 Introduction

Since 2006 Saab Aerosystems has been developing the unmanned autonomous helicopter Skeldar. The helicopter is designed for both military and commercial applications with VTOL and hovering capacity. The present paper focus on an early version of the helicopter V150 (see fig 1). The outline of the paper is the following. In section 2 the flight mechanical models are discussed, the use of symbolic calculation, which is an essential part for deriving the different models, is presented in section 3. Section 4 and 5 consider black box modelling and the design of control laws and simulation results are finally discussed in section 6.

Fig 1. The autonomous helicopter Skeldar V150

2 Flight mechanical models

The different parts in the dynamical flight mechanical model are described in this section. The models are divided in four parts, the main and tail rotor models i.e. the helicopter blade motion and forces, the paddle model and the rigid body model.

2.1 The helicopter blade dynamics

We will in this section describe how the helicopter blade motion can be derived using a number of general coordinate transformations for rigid bodies. The main reason for using this approach is that symbolic mathematical software can be directly applied. Hence the derivation and simplification of the equation is done automatically which reduces the risk for introducing errors in the model and the final computer code. The transformations we are going to use go from an earth fixed coordinate system (*E*), via the helicopter body (*B*) and the helicopter hub (*H*) to the helicopter blade (*b*) system. These transformations are mathematically described by following equations.

$$\begin{aligned} x_E &= x_{B,0} + T_{E2B} x_B \\ x_B &= x_{H,0} + T_{B2H} x_H \\ x_H &= x_{b,0} + T_{H2b} x_b \end{aligned} \qquad (1)$$

The transformation notation *E2B* denotes a coordinate transformation from the body to earth system. Differentiating (1) with respect to the time and using the fact that $\dot{T}_{B2H} = \dot{x}_b = \ddot{x}_b = 0$ leads to

$$\begin{aligned} \ddot{x}_E &= \ddot{x}_{B,0} + T_{E2B}\left(\omega_B \times (\omega_B \times x_B)\right) + \\ & T_{E2B}\left(\dot{\omega}_B \times x_B + 2\omega_B \times \dot{x}_B + \ddot{x}_B\right) \\ \ddot{x}_B &= T_{B2H}\ddot{x}_H \\ \ddot{x}_H &= \ddot{x}_{b,0} + T_{H2b}\left(\omega_b \times (\omega_b \times x_b)\right) + \\ & T_{H2b}\left(\dot{\omega}_b \times x_b\right) \end{aligned} \qquad (2)$$

where ω_B and ω_b are the angular velocities of the helicopter body and the helicopter blade respectively. Equation (2), which describes the acceleration of a point on the helicopter blade, in three different coordinate systems, can be simplified furthermore by assuming that the helicopter body acceleration is small compared to the helicopter blade acceleration i.e. $\ddot{x}_{B,0} = \omega_B \times (\omega_B \times x_B) = \dot{\omega}_B \times x_B \approx 0$ .This implies, after further simplifications of (2),

$$\begin{aligned} T_{b2H}T_{H2B}T_{B2E}\ddot{x}_E &= T_{b2H}T_{H2B}\left(2\omega_B \times \dot{x}_B\right) + \\ T_{b2H}\ddot{x}_{b,0} &+ \omega_b \times (\omega_b \times x_b) + \dot{\omega}_b \times x_b \end{aligned} \qquad (3)$$

Assuming that the earth coordinate system is an inertial frame in which Newton's second law holds at the point x_E we have

$$\rho \ddot{x}_E = f_E \qquad (4)$$

where ρ is the density of the helicopter blade and f_E the force which can alternatively be written $f_E = T_{E2B}T_{B2H}T_{H2b} f_b$. Inserting (4) into (3) results in

$$\begin{aligned} \rho\dot{\omega}_b \times x_b &= f_b - \rho T_{b2H}T_{H2B}\left[2\omega_B \times \dot{x}_B\right] - \\ & \rho\left[T_{b2H}\ddot{x}_{b,0} + \omega_b \times (\omega_b \times x_b)\right] \end{aligned} \qquad (5)$$

The term $\rho T_{b2H}T_{H2B}\left[2\omega_B \times \dot{x}_B\right]$ can be interpreted as the gyroscopic force and $\rho\left[A_{h2b}\ddot{x}_{b,0} + \omega_b \times (\omega_b \times x_b)\right]$ as the centrifugal force. The force f_b in equation (5) is needed when computing the forces on the helicopter body $F_{B,mnr}$ and $F_{B,tlr}$, from the main and tail rotor. (see next section 2.2). I the remaining part of this section we will derive equations from which ω_b can be computed. Multiplying both sides in (5) by $x_b \times$ and integrating over the blade yields

$$\begin{aligned} & I_b\dot{\omega}_b + \omega_b \times (I_b\omega_b) = M_b - \\ & \iiint \rho x_b \times \left(T_{b2H}T_{H2B}\left[2\omega_B \times \dot{x}_B\right] - T_{b2H}\ddot{x}_{b,0}\right) \end{aligned} \qquad (6)$$

where I_b is the moment of inertia and M_b the torque around the hinge (see fig.2). From (6) we obtain three decoupled equations for the blade flapping (β) the pitching (θ) and the lead/lag (ξ) motion.

$$\ddot{\beta}+\frac{2+e}{2(1-e)}\Omega^2\beta+\frac{2+e}{(1-e)}(-p\cos(\Omega t)+q\sin(\Omega t))=\frac{M_{b,\beta}}{I_\beta}$$
$$\ddot{\theta}+\Omega^2\theta+2\Omega(p\sin(\Omega t)+q\cos(\Omega t))=\frac{M_{b,\theta}}{I_\theta}$$
$$\ddot{\xi}+\frac{3e}{2(1-e)}\Omega^2\xi=\frac{M_{b,\xi}}{I_\xi} \qquad (7)$$

where

$$I_\beta=\frac{1}{3}m_bR^2(1-e)^2,\quad I_\theta=\frac{1}{12}m_bc^2$$
$$I_\xi=\frac{1}{12}m_b\left(4R^2(1-e)^2+c^2\right) \qquad (8)$$

and R is the radius of the propeller disc, c the chord of the blade, $R(1-e)$ the length of the blade, m_b the blade mass and p,q the angular speed of the helicopter. The equations above are solved in the following steps

1. Solve the β equation in (7).
2. The pitching angle θ is known from the forced blade pitching so no equation need to be solved.
3. The lead/lag ξ is neglected in the present paper.
4. The angular speed ω_b is computed from β and θ.
2. Compute equation f_b from equation (5).
3. Compute the hinge forces $F_{B,mnr}$.

The equations above are valid for both the main and the tail rotor.

2.2 The helicopter blade forces

This section describes how the forces and moments on the rotor blades are computed. The aerodynamic force on the blade, which is the essential force, is obtained from lift and drag force on the blade according to (9)

$$F_b=\iint f_b dS=\int[(D\cos\phi+L\sin\phi,0,L\cos\phi-D\sin\phi)]dy \qquad (9)$$

The local lift (L) and drag (D) yield

$$L=\frac{1}{2}\rho U^2c\bullet c_{l,\alpha}\bullet\left(\underbrace{\theta+\phi-\alpha_0}_{\alpha}\right)$$
$$D=\frac{1}{2}\rho U^2c\bullet c_d \qquad (10)$$

The moment around the hinge (i.e. $x_b=0$ in the blade system) can be written

$$M_b=\iint x_b\times f_b dS \qquad (11)$$

Which can be expressed, using the lift and drag above, as

$$M_b=\int\begin{bmatrix}y(L\cos\phi-D\sin\phi)\\-x_{b,cp}(D\cos\phi+L\sin\phi)\\-y(D\cos\phi+L\sin\phi)\end{bmatrix}dy \qquad (12)$$

The torque contribution, from the main and tail rotor, onto the helicopter body, can now be obtained from (10) and (12) according to

$$M_{B,mnr}=M_b+\Delta l\times F_b \qquad (13)$$

Where Δl is the distance vector from the rotor shaft to the blade hinge (see fig 2).

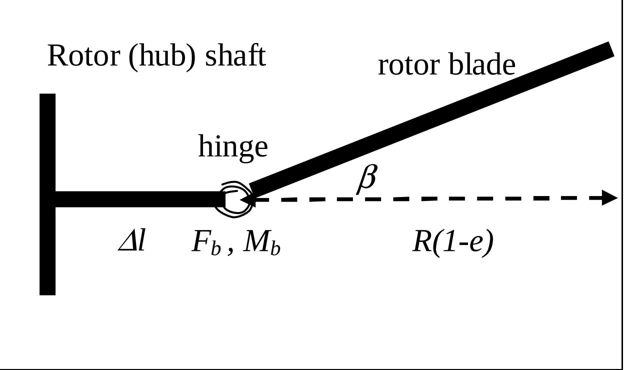

Fig 2. Generic helicopter blade

2.3 The helicopter paddle dynamics

The Skeldar helicopter V150 has stabilizing paddles (a Bell-Hiller mixer) which control the helicopter blade motion. The paddle motion is modeled in a similar way as the motion of the helicopter blades above.

To close the blade and paddle equations we need to describe the coupling to swash plate and linkage between the swash plate and the paddles/rotor blades.

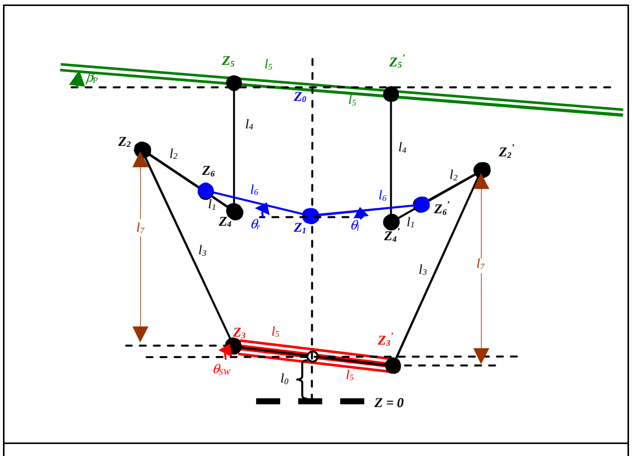

Fig 3. Bell-Hiller mixer including linkage, the connecting the flybar, the swashplate and the main rotor blade grip

We can establish three identities, which define the relation between Bell-Hiller bar angle β_P, the swash plate angles $\theta_0, \theta_c, \theta_s$ and the pitch angles of the individual blades θ_1, θ_2.

$$\theta_1 = \theta_0 + f_1 \cdot (-\theta_c \cdot \sin\psi + \theta_s \cdot \cos\psi) + f_2 \cdot \beta_P$$
$$\theta_2 = \theta_0 - f_1 \cdot (-\theta_c \cdot \sin\psi + \theta_s \cdot \cos\psi) - f_2 \cdot \beta_P$$

For the collective pitch θ_0 holds $\theta_0 = f_0 l_0$. The factors f_0, f_1 and f_2 are constants depending only on the ratio between the length of the rods involved in the Bell-Hiller mixer (see fig.3).

2.4 Rigid body model

The general equations of a rigid body motion, which can be found in a standard text book in solid mechanics, are applied to the helicopter body

$m\ddot{x}_{CG} = F_B$	(14)

where x_{CG} is the center of gravity, *m* the mass and F_B is the total forces on the helicopter. The corresponding equation for angular velocity ω_B reads

$I\dot{\omega}_B + \omega_B \times (I\omega_B) = M_B$	(15)

where M_B is the total torque on the helicopter. We will in the next section describe how the total force and torque are computed.

2.5 Forces and torque on the helicopter

The forces and torque acting on the helicopter are split up in four parts

$F_B = F_{B,mnr} + F_{B,tlr} + F_{B,aero} + F_{B,gravity}$	(16)

$M_B = M_{B,mnr} + M_{B,aero} + M_{B,tlr} +$ $(x_{CG} - x_{mnr}) \times F_{B,mnr} + (x_{CG} - x_{tlr}) \times F_{B,tlr}$	(17)

where the subscripts *mnr* denotes the main rotor, *tlr* the tail rotor and *aero* aerodynamic forces. The forces and torque from the main and tail rotor are obtained from the equations in section 2.2 above. The aerodynamic forces and moments are obtained from CFD computations and handbook methods.

3 Symbolic computations using Maple

As have been mentioned in the previous sections the approach for deriving the different models in the present paper is well suite for symbolic operation. We have for this purpose used the well known Symbolic Computation System Maple. Different tools for simplifying, expanding, developing multi Taylor series, etc. were applied to the mathematical expressions derived above. In this way mistakes and calculation error were avoided and a lot of cumbersome hand calculations were saved. The equations describing the dynamical equations and the forces and moments are rather complicated and difficult to implement efficiently in a computer program. Since the final code was aimed at real time simulations it was hence important to write the code in very efficient way. This was achieved using the Maple code generation library together with own developed MATLAB codes. The Maple soft ware was also used to generate a linearized version of the simulation software which is of importance for the development of control laws.

4 The black box model

In parallel to the development of the flight mechanical model described above, a black box model of the rotational and translational dynamics has been developed using system identification. The term black box refers to that this model has been derived using no (or at least minimal) physical insight into the helicopter dynamics.

The core idea in system identification is to construct a dynamic model directly from data collected from running the system. In this project, flight tests have been designed and performed to collect data from pitch, roll, yaw and climb maneuvers starting from a hovering condition.

Low order linear dynamic models have then been fitted to these data. Typically, several model structures (in terms of input and output signals) and model orders are tested to come up with the “best” model. In this context, a “good” model is a model of low order with few input signals that can reproduce the observed output data well. The standard estimation-validation data split has been performed to test the accuracy and the predictive strength of the models.

Since the performed maneuvers are rather short and since the dynamic range of the sensors is limited, the resulting models will only capture the helicopter dynamics in a mid-frequency range. For control purposes, this is precisely the frequency range of interest since very fast dynamics (e.g., some of the dynamic modes of the rotors) can be approximated as being infinitely fast, and very slow dynamics (e.g., the phugoid like modes of the body movement) will be stabilized automatically when closing the loop with a controller.

5 Control laws

In the Skeldar flight control system, there are several different autonomous control modes, e.g., for hovering, for forward flight and for take-off and landing. The core control mode is the hover mode, the other modes are derivates of this mode.

In hover, the control objective is to maintain a user commanded horizontal position, altitude and heading in the presence of wind disturbances.

To sense the helicopter state, an integrated AHRS/GPS unit is used that continuously reports the position, velocity, orientation, angular velocity and acceleration (all 3-D vectors) of the helicopter. After filtering out some narrowband noise, due to the engine and the rotors, these signals are used for feedback.

The feedback controller is composed by separate SISO (single input, single output) controllers for forward positioning, lateral positioning and for altitude and heading control. Hence, the dynamic couplings that exist between, e.g., the pitch and roll dynamics, are ignored by the controller. Such approximations are vital to make to come up with a controller with a simple structure.

In each degree of freedom (forward, lateral, vertical, heading), the controller consists of a “multivariable” PI controller, with proportional feedback from the relevant sensor signals and integral control of the signal related to one of the hovering control objectives.

For example, the heading control loop consists of proportional feedback from yaw rate and heading error together with integral feedback of the heading error. The proportional parts add virtual damping to the system and the integral part accomplishes automatic trim of the tail rotor.

The controller parameters are computed using linear-quadratic (LQ) optimal control. In theory, this gives the closed loop system certain robustness properties such as 60 degrees phase margin and infinite gain margin at the input of the plant. In practice, these margins are reduced somewhat due to some of the simplifying model assumptions that are made, e.g., neglecting certain fast rotor dynamics and also couplings between motion around different axes. However, LQ still provides the control designer with a very useful and intuitive tool for designing robust control laws with a “natural” transient response.

In pitch, roll and climb, the control commands computed by the feedback loops are distributed to the individual main rotor servos based on the geometry of the swashplate.

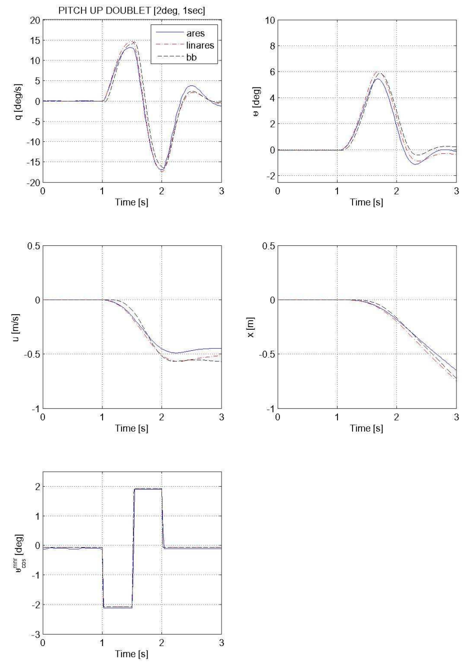

Fig 4. Comparison of the longitudal motion

6 Results

The fully nonlinear simulation model above, a linearized version of this model and the black box model have been compared and validated. Samples from this validation study are shown in figure 4 and 5. Figure 4 shows comparison of the pitching motion, starting from a trimmed hovering state, from an input signal corresponding to a doublet in $\theta_{\cos}$ of the main rotor swash plate. In figure 5 has instead a doublet in $\theta_{\sin}$ of the main rotor swash plate been applied. Both test cases show a good agreement between the three models as can be seen in figure 4 and 5.

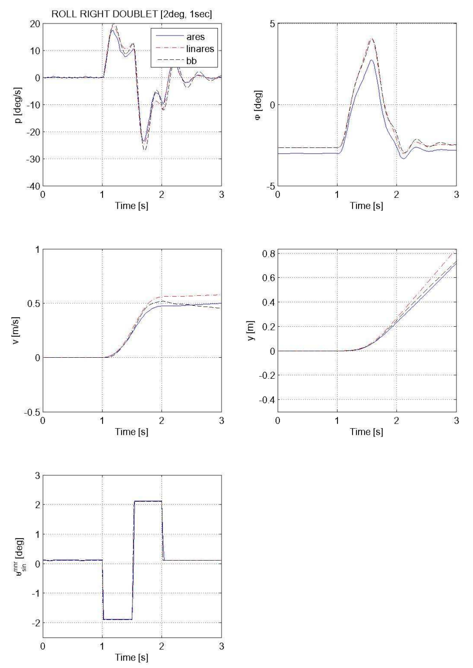

Fig. 5 Comparison of the lateral motion

7 References

[1] Leischman *Principles of Helicopter Aerodynamics.* 2nd edition, Cambridge University Press, 2006.

[2] Bramwell A. R. S, Done G. and Balmford D. *Helicopter Dynamics* 2nd edition, Butterworth-Heinemann , 2001.

Copyright Statement